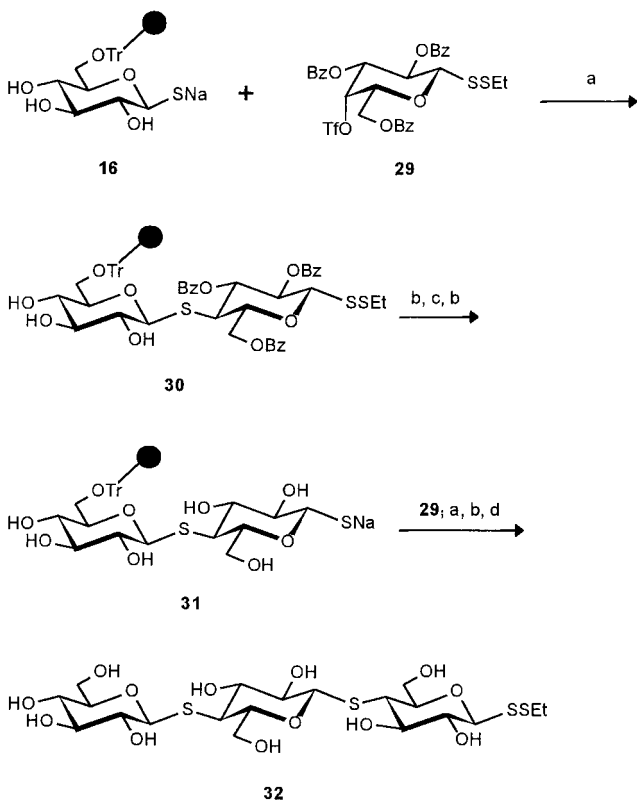


Table 1. Selected ^1H NMR signals (360 MHz, CD_3OD) and MS data of **20**, **22–28**, and **32**.

20 : $\delta = 4.35$ (d, 1H, $J_{1,2} = 9.7$ Hz; 1b-H, 1c-H), 5.45 (d, 1H, $J_{1,2} = 5.0$ Hz; 1a-H); MS: m/z : 461.2 [$M^+ - \text{Na}$]
22 : $\delta = 4.18$ (d, 1H, $J_{1,2} = 7.6$ Hz; 1b-H), 4.42 (d, 1H, $J_{1,2} = 9.6$ Hz; 1a-H); MS: m/z : 493.2 [$M^+ - \text{Na}$]
23 : $\delta = 4.40$ (d, 1H, $J_{1,2} = 9.6$ Hz; 1b-H), 5.45 (d, 1H, $J_{1,2} = 5.0$ Hz; 1a-H); MS: m/z : 461 [$M^+ - \text{Na}$]
24 : $\delta = 4.18$ (d, 1H, $J_{1,2} = 7.6$ Hz; 1a-H), 4.48 (d, 1H, $J_{1,2} = 9.7$ Hz; 1b-H); MS: m/z : 493.2 [$M^+ - \text{Na}$]
25 : $\delta = 4.55$ (d, 1H, $J_{1,2} = 10.3$ Hz; 1b-H), 5.45 (d, 1H, $J_{1,2} = 5.0$ Hz; 1a-H); MS: m/z : 502.2 [$M^+ - \text{Na}$]
26 : $\delta = 4.16$ (d, 1H, $J_{1,2} = 7.6$ Hz; 1a-H), 4.70 (d, 1H, $J_{1,2} = 10.4$ Hz; 1b-H); MS: m/z : 534.3 [$M^+ - \text{Na}$]
27 : $\delta = 1.31, 1.33, 1.39, 1.49$ ($4 \times \text{s}$, 12H; CH_3), 1.80 (dd, 1H, $J_{3a,4} = 11.3$, $J_{3a,3e} = 12.8$ Hz; 3b-H _a), 1.98 (s, 3H; NCOCH_3), 2.75 (dd, 1H, $J_{3e,4} = 4.6$, $J_{3e,3a} = 12.8$ Hz; 3b-H _e), 3.67 (s, 3H; COOCH_3), 4.31 (dd, 1H, $J_{1,2} = 5.0$, $J_{2,3} = 2.4$ Hz; 2a-H), 4.61 (dd, 1H, $J_{2,3} = 2.4$, $J_{3,4} = 7.9$ Hz; 3a-H), 5.42 (d, 1H, $J_{1,2} = 5.0$ Hz; 1a-H); MS: m/z : 604.2 [$M^+ - \text{Na}$]
28 : $\delta = 0.88$ (m, 3H; CH_3), 1.28 (m, 10H; Octyl), 1.56 (m, 2H; OCH_2CH_2), 1.99 (s, 3H; NCOCH_3), 1.79 (dd, 1H, $J_{3a,4} = 11.3$, $J_{3a,3e} = 12.8$ Hz; 3b-H _a), 1.97 (s, 3H; NCOCH_3), 2.75 (dd, 1H, $J_{3e,4} = 4.6$, $J_{3e,3a} = 12.8$ Hz; 3b-H _e), 3.67 (s, 3H; COOCH_3), 4.20 (d, 1H, $J_{1,2} = 7.6$ Hz; 1a-H); MS: m/z : 636.3 [$M^+ - \text{Na}$]
32 : $\delta = 1.30$ (t, 3H, $J = 7.4$ Hz; CH_3), 2.83 (q, 2H, $J = 7.4$ Hz; SCH_2), 4.31 (d, 2H, $J_{1,2} = 9.3$ Hz; 1b-H, 1c-H), 4.40 (d, 1H, $J_{1,2} = 9.5$ Hz; 1a-H); MS: m/z : 635.1 [$M^+ - \text{Na}$]



Scheme 5. a) $[15]\text{Crown-5}$, THF, 20°C , 16 h; b) NaOMe , MeOH , THF; c) DTT, THF, MeOH , Et_3N ; d) TFA, CH_2Cl_2 , 20°C .

firmly that O-glycosidic bond cleavage from the resin was in fact responsible for the lower yields of about 70% found for compounds **20–28**.

In conclusion, a highly efficient method for the synthesis of thio-oligosaccharides on the solid-phase has been described.

All glycosides were obtained stereoselectively and in high yield. Side products arising from elimination of the triflates could be easily removed by washing the resin after glycosylation. The protection of the anomeric thiol function as an ethyl disulfide proved to be compatible with common carbohydrate reaction conditions and served as an ideal protective group.

Received: November 6, 1998 [Z12628IE]
German version: *Angew. Chem.* **1999**, *111*, 1900–1902

Keywords: oligosaccharides • solid-phase synthesis • thio-glycosides • thiolates • thio-oligosaccharides

- a) Z. J. Witczak, R. Chhabra, H. Chen, X.-Q. Xie, *Carbohydr. Res.* **1997**, *301*, 167–175; b) F. Shafizadeh, R. H. Furneaux, T. T. Stevenson, *Carbohydr. Res.* **1979**, *71*, 169–191.
- L. A. Reed, L. Goodman, *Carbohydr. Res.* **1979**, *94*, 91–99.
- L. X. Wand, N. Sakari, H. Kuzuhara, *J. Chem. Soc. Perkin Trans. 1* **1990**, 1677–1682.
- T. Eisele, A. Toepfer, G. Kretzschmar, R. R. Schmidt, *Tetrahedron Lett.* **1996**, *37*, 1389–1392.
- Z. J. Witczak, J. M. Sun, R. Mielgaj, *Bioorg. Med. Chem. Lett.* **1995**, *5*, 2169–2174.
- V. Moreau, J. C. Norrild, H. Driguez, *Carbohydr. Res.* **1997**, *300*, 271–277.
- T. Mukaiyama, K. Takahashi, *Tetrahedron Lett.* **1968**, 5907–5908.
- a) D. Horton, *Methods Carbohydr. Chem.* **1963**, *2*, 433–437; b) D. Zanini, W. K. C. Park, R. Roy, *Tetrahedron Lett.* **1995**, *36*, 7383–7386; c) W. K. C. Park, S. J. Meunier, D. Zanini, R. Roy, *Carbohydr. Lett.* **1995**, *1*, 179–184; R. Roy, D. Zanini, S. J. Meunier, A. Romanowska, *J. Chem. Soc. Chem. Commun.* **1993**, 1869–1872.
- D. Horton, *Methods Carbohydr. Chem.* **1972**, *6*, 282–285.
- The resin is commercially available from Novabiochem. Immobilization was performed by using pyridine as solvent in the presence of 4-dimethylaminopyridine (DMAP) for 48 h at 60°C .
- Yield of isolated product. The isopropylidene groups of **20**, **23**, **25**, **27** and the O-glycosidic bonds of unprotected **22**, **24**, **26**, **28** were partly cleaved under acidic conditions. Cleaving the benzoyl-protected thiodisaccharides from the resin afforded the corresponding disaccharides in quantitative yields since the presence of the electro-negative benzoyl esters stabilizes the glycosidic linkages. The use of more acid labile linker systems is currently under investigation.

Characterization of Ligand Binding by Saturation Transfer Difference NMR Spectroscopy**

Moriz Mayer and Bernd Meyer*

The difference between a saturation transfer spectrum and a normal NMR spectrum provides a new and fast method (saturation transfer difference (STD) NMR spectroscopy) to

[*] Prof. Dr. B. Meyer, Dipl.-Chem. M. Mayer
Institut für Organische Chemie der Universität
Martin-Luther-King-Platz 6, D-20146 Hamburg (Germany)
Fax: (+49) 40-42838-2878
E-mail: bernd.meyer@sg1.chemie.uni-hamburg.de
moriz.mayer@sg1.chemie.uni-hamburg.de

[**] Support by the Bundesministerium für Bildung und Forschung, Bruker Analytik GmbH, and the Deutsche Forschungsgemeinschaft (program project grant SFB 470 and GRK 464) is acknowledged.

screen compound libraries for binding activity to proteins. STD NMR spectroscopy of mixtures of potential ligands with as little as 1 nmol of protein yields 1D and 2D NMR spectra that exclusively show signals from molecules with binding affinity. In addition, the ligand's binding epitope is easily identified because ligand residues in direct contact to the protein show much stronger STD signals. For example, the binding specificity of Lewis^b-hexasaccharide to *Aleuria aurantia* agglutinin (AAA) can be mapped to the two fucosyl residues.

Identification of the binding activity and characterization of the binding epitope of ligands to proteins is important in biochemical and pharmaceutical research. The advantage of NMR-based techniques in comparison to other screening methods in use today, such as ELISA, RIA, Biacore, or immunoblotting, is the possibility of directly identifying the binding component from a mixture of potential ligands. Any small molecule in solution reversibly interacting with the binding domain of a protein shows characteristic differences in its relaxation behavior and molecular mobility from those molecules having no affinity for the protein. Transferred NOE spectra,^[1] diffusion- or relaxation-edited NMR spectra,^[2] as well as ¹⁵N chemical shift studies^[3] were used to identify substances with binding affinity from compound mixtures. The factors that reduce the utility of NMR methods for high-throughput screening are relatively long acquisition times and the dependence on ligand excess. An additional drawback of the ¹⁵N chemical shift technique is the need for large quantities of valuable ¹⁵N-labeled biomolecules and the limitation on the protein size to <30 kDa.^[3] Spin diffusion experiments have to date been used in a variety of ways such as the study of motional properties of proteins,^[4] the effect of H₂O suppression on NMR spectra,^[5] and the study of ligand–protein interactions.^[6]

Macromolecules, like proteins, consist of a large system of protons tightly coupled by dipole–dipole interactions.^[7] The longitudinal relaxation rate R_1 of protons in proteins is dominated by the cross relaxation rate σ_{intra} . Selective saturation of a single protein resonance will result in a rapid spread of the magnetization over the entire protein (spin diffusion). Intramolecular transfer of magnetization from protein to ligand (σ_{inter}) leads to progressive saturation of the ligand (Figure 1). The only limitation imposed on molecules in the mixture is that they must not be affected by the selective saturation pulse. The NOE pumping method^[2b] also relies on the transfer of polarization from the receptor to the bound compound. In contrast to the NOE pumping method, STD NMR spectroscopy does not require a diffusion filter, and the NOE mixing (pumping) time is replaced by the selective saturation time. These factors make STD NMR spectroscopy more sensitive and flexible in its applications. STD NMR spectroscopy should enable the identification of ligand binding to proteins with dissociation constants K_D between 10^{-3} and 10^{-8} .^[8]

The efficiency of the STD NMR technique is shown by the binding of *N*-acetylglucosamine (GlcNAc) to wheat germ agglutinin (WGA). Other studies have shown that the lectin receptor has an affinity for this ligand.^[9] We composed a library containing six nonbinding saccharides additional to the binding monosaccharide GlcNAc. Figure 2A shows the 1D

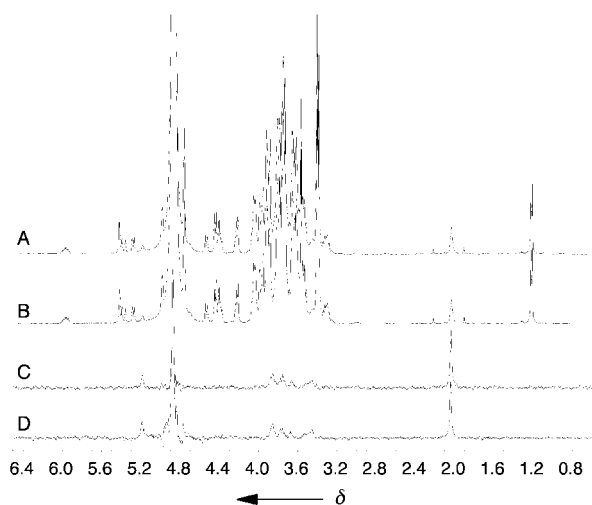
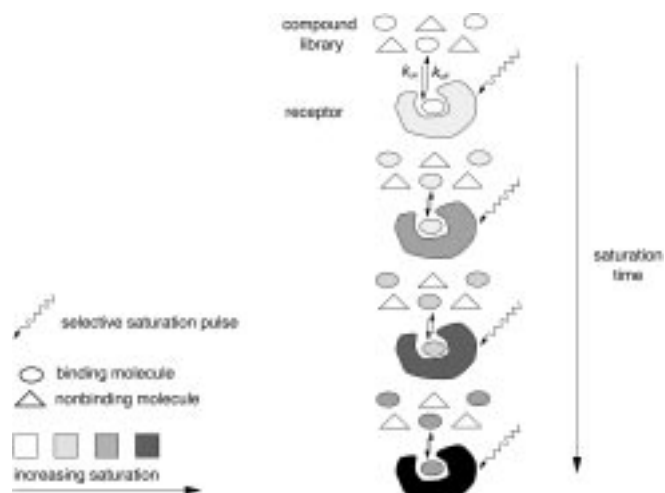


Figure 2. Characterization of ligands with binding affinity with the 1D STD NMR spectroscopic method. A) 1D ¹H NMR spectrum of a mixture of seven saccharides (1 mM of α -D-GlcNAc, α -D-Man-OMe, α -D-Gal-OMe, α -L-Fuc-OMe, β -D-Gal-(1 \rightarrow 4)- β -D-Glc-OMe, β -D-Gal-(1 \rightarrow 4)- β -D-Glc-O-Allyl, D-raffinose) and WGA recorded with off-resonance irradiation at $\delta = 30$, and B) with on-resonance irradiation at $\delta = 10$. C) The corresponding STD spectrum (spectrum (A) minus spectrum (B)). D) Reference spectrum showing a STD NMR spectrum obtained from WGA and GlcNAc alone without the six nonbinding saccharides. The spectra (C) and (D) were obtained by collecting 128 scans for the on- and off-resonance spectra each and internal subtraction from each other by phase cycling. Only resonances of GlcNAc remain in the STD NMR spectra (C) and (D). The concentration of WGA in solution was 45 μ M (binding sites), the excess of the ligands was about 20:1. A pulse train of 40 Gaussian bell-shaped selective pulses of 50 ms duration separated by a 1 ms delay were used to saturate the protein. A T_2 relaxation filter consisting of a 70 ms spin lock pulse was applied to remove protein background signals resulting also in reduced signal intensities in (C) and (D).

^1H NMR spectrum^[10] of the compound library recorded with off-resonance irradiation at $\delta = 30$. Figure 2B shows the 1D ^1H NMR spectrum of the same sample with selective saturation of the protein by a cascade of shaped pulses with on-resonance irradiation at $\delta = 10$. One can clearly see that the binding compound cannot be identified by observing changes of intensity between the spectra (A) and (B) due to extreme overlap in the hump region (ring protons) (Figure 2). However, in the difference spectrum given in Figure 2C even signals of the hump region may be assigned, making identification of GlcNAc possible. For reference, the STD NMR spectrum in Figure 2D was recorded with a sample containing WGA in the presence of only GlcNAc. The spectra in Figures 2C and 2D are identical proving that all signals from non-binding compounds are completely eliminated in Figure 2C.

The dependence of the degree of saturation on ligand excess was determined by titration of GlcNAc relative to WGA (Figure 3A). The signal-to-noise ratio determined

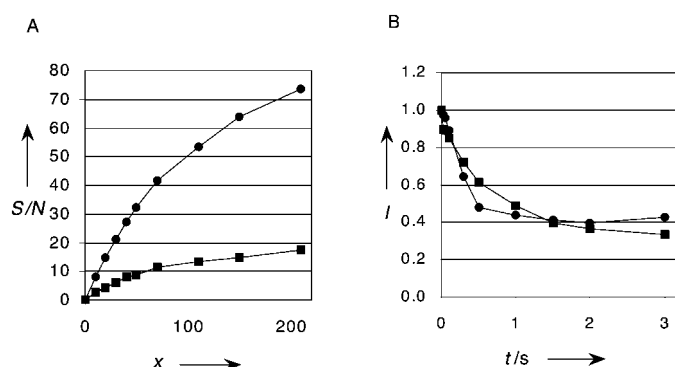


Figure 3. A) Signal-to-noise ratio (S/N) obtained from STD NMR spectra as a function of the molar excess (x) of GlcNAc relative to WGA for selected resonances (\bullet N -acetyl group, \blacksquare α -H1). The sample contained 22 nmol WGA. The spectra were recorded at 290 K with off-resonance irradiation at $\delta = 20$ and on-resonance irradiation at $\delta = 7$. Maximum saturation is not even reached at a 200-fold molar excess of ligand. B) Integral value (I) as a function of saturation duration (t) of selected α -L-Fuc-OMe resonances (\bullet O -methyl group, \blacksquare H6-Fuc group). The sample contained 28 nmol of AAA and a 30-fold molar excess of ligand. The spectra were recorded at 310 K with selective irradiation of the protein at $\delta = 7$. Saturation of signals increases to about 2 s leveling out at about 60% reduction of signal intensity.

from difference spectra of the anomeric α -H1 proton and the N -acetyl group increases beyond an excess of 210:1. The intensity of the STD NMR signal increases as a function of ligand excess as long as ligand molecules having received no or little saturation bind to the receptor. Therefore, high turnover rates result in a larger effect at higher ligand-to-protein ratios. Slow dissociation rates will yield smaller STD NMR signals and, thus, reduce sensitivity.

Figure 3B indicates the dependence of the STD NMR signal intensity on the duration of saturation. The saturation profile shows that intra- and intermolecular saturation transfer is very efficient since a 100 ms irradiation period leads to a decrease in signal intensity of ligand resonances by about 15%. The maximum degree of saturation under these conditions of about 60% is reached at a saturation time of about 1.5 s. More important in this context is that prolonged irradiation of the protein does not lead to a decrease of the STD NMR signal intensity. The high degree of saturation

(60%) even at a ligand excess of 30:1 makes STD NMR spectroscopy very sensitive and, therefore, only very small amounts of protein are required. In sum, the degree of saturation of ligands depends on the size of the protein, the offset, and the duration of the on-resonance irradiation, the dissociation rate constant k_{off} , and the excess of ligand.

Screening of the library containing 22 nmol (400 μg) of WGA and a 20-fold ligand excess by 1D STD NMR spectroscopy is possible in two minutes. The sensitivity limits of the method became apparent when we successfully observed GlcNAc binding to as little as 1 nmol of WGA (18 μg) from a mixture of 200 nmol GlcNAc (44 μg) and α -L-Fuc-OMe (36 μg) each within about one hour on a 500 MHz spectrometer. Using higher field spectrometers will make the method even more efficient since sensitivity and spin diffusion increase with field strength.

To identify more complex components from a library additional experiments, that is 2D NMR spectra, are necessary. The saturation transfer effect is applicable to virtually any form of NMR experiment. This allows us to record 2D experiments that reveal structural information of the ligand interacting with the protein. Here, we demonstrate the benefits of STD NMR spectroscopy by means of a TOCSY difference spectrum (Figure 4) with the same NMR sample

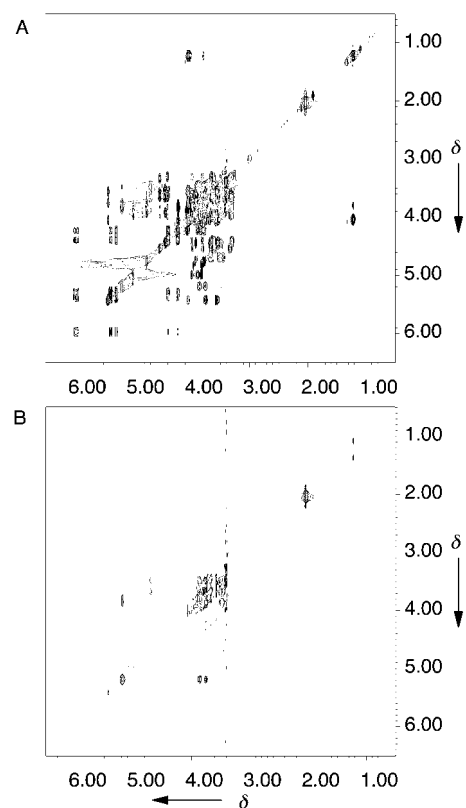
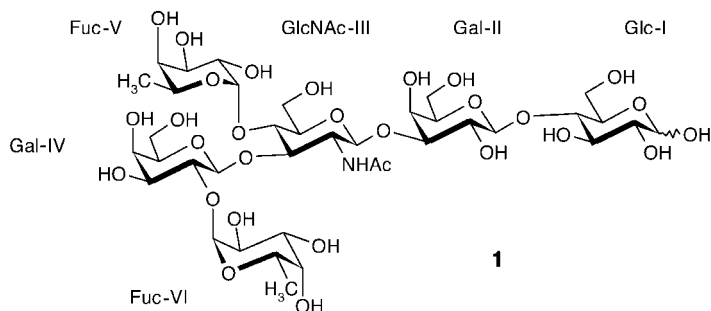


Figure 4. Characterization of ligands with binding affinity with the 2D STD NMR spectroscopic method. A) TOCSY spectrum of a mixture of seven saccharides and WGA recorded with off-resonance irradiation at $\delta = 20$. B) STD TOCSY spectrum obtained by subtraction of a spectrum recorded with on-resonance irradiation at $\delta = 7$ from spectrum (A). The on- and off-resonance TOCSY spectra were recorded at 290 K with 200 increments in t_1 and 32 transients each. Only resonances of GlcNAc remain in the STD TOCSY spectrum. The two spectra were recorded with t_1 increments interlaced and processed and phased identically before subtraction.

used in the 1D experiment. The spectrum in Figure 4 A shows the TOCSY spectrum of the compound mixture recorded with off-resonance irradiation. Figure 4 B shows the STD TOCSY spectrum containing only cross peaks originating from the binding component GlcNAc. The recording of 2D NMR spectra allows unambiguous identification of complex ligand molecules directly from mixtures.

To test the STD NMR spectroscopic method with a larger ligand we recorded TOCSY spectra of Lewis^b-hexasaccharide (lacto-*N*-difucosylhexaose I, **1**) in presence of the fucose-



binding lectin AAA.^[11] The resonances of the individual sugar residues of the Lewis^b-hexasaccharide show very different intensities (Figure 5). Only the fucose residues are located in direct contact to the protein and, thus, obtain a high degree of saturation directly from the protein (Figure 5 B). The other sugar residues, namely Gal-II, GlcNAc-III and Gal-IV, show only about 60 % of the saturation since they can only obtain saturation through the directly interacting fucoses (Figure 5 C). The Glc-I residue shows an even smaller effect of about 30 % saturation relative to that of the fucosyl residues (not shown). Therefore, binding epitope and neighboring residues can easily be mapped by STD NMR spectroscopy. This holds true for all ligands where the transfer of magnetization outside the binding epitope goes through a “bottle-neck” such as peptide^[12] or glycosidic linkages. The analysis shown here was made with 10 nmol of recoverable protein and 1 μ mol of ligand. Therefore, STD NMR spectroscopy seems to be a viable alternative to, for example, mapping of binding epitopes by determining the affinity of a large number of short overlapping peptides by ELISA.

In conclusion, STD NMR spectroscopy is a new member of bioaffinity NMR methods^[1a,b] which allow detection and identification of binding molecules directly from mixtures. It is insensitive to ligand excess and eliminates the risk of detecting false positives, since only saturation transferred to the ligand through the protein is detected. With STD NMR spectroscopy there are few limitations to the size of the ligand molecules as long as the receptor can be selectively excited. Compound mixtures containing substances in variable concentrations and of different sizes can therefore be efficiently screened. Furthermore, there is no limit to the size of the protein. In fact, there is an increase of sensitivity with the size of protein due to a more efficient inter- and intramolecular saturation transfer. In contrast to the determination of structure–activity relationships (SAR) by NMR spectroscopy this method does not yield information on the receptor site of the protein. STD NMR spectroscopy should also be appli-

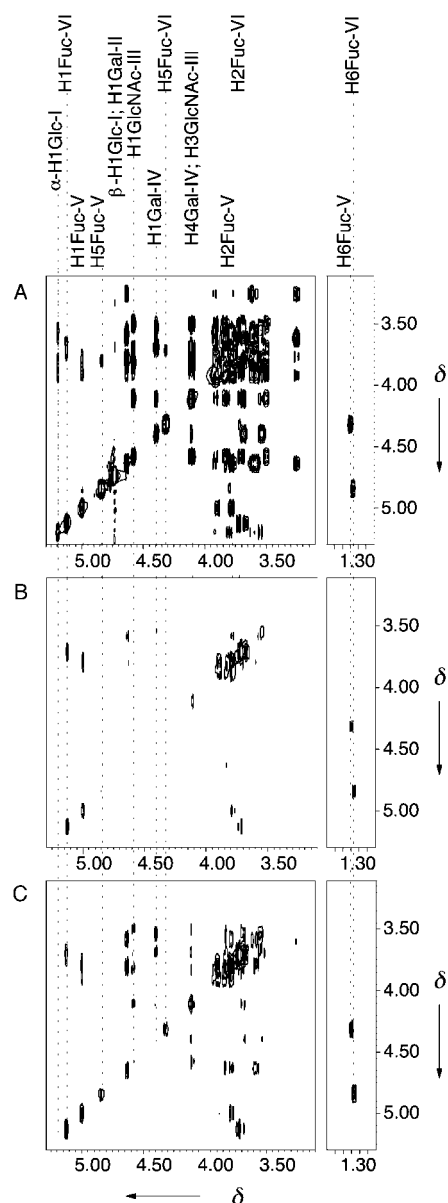


Figure 5. STD NMR TOCSY spectra of Lewis^b-hexasaccharide demonstrating epitope mapping. A) TOCSY spectrum of **1** without protein. B) STD TOCSY spectrum of **1** in the presence of the protein AAA (10 μ M binding sites) showing only the intensive signals of fucosyl residues V and VI. C) STD TOCSY spectrum at about 60 % level of that in (B) showing in addition to the fucosyl cross peaks from (B) cross peaks originating from Gal-II, GlcNAc-III, and Gal-IV. The full STD TOCSY exhibiting also the even less intensive signals of Glc I at about 30 % of the intensity of cross peaks in (B) is not shown. The on- ($\delta=10$) and off-resonance ($\delta=30$) TOCSY spectra were recorded at 300 K with 200 increments in t_1 and 40 transients each.

cable to tighter binding ligands although the absolute effect will be smaller than with faster exchanging ligands since fewer ligands are saturated and exchanged into solution. Very valuable is the fact that most 1D or nD experiments can be modified in such a way that the STD NMR method is applicable, for example TOCSY, COSY, NOESY, and inversely detected ¹³C or ¹⁵N spectra.

Received: January 8, 1999 [Z12885 IE]
German version: *Angew. Chem.* **1999**, *111*, 1902–1906

Keywords: bioaffinity studies • combinatorial chemistry • molecular recognition • NMR spectroscopy

A Solution-Phase Chemical Approach to a New Crystal Structure of Cobalt**

Dmitry P. Dinega and M. G. Bawendi*

- [1] a) B. Meyer, T. Weimar, T. Peters, *Eur. J. Biochem.* **1997**, *246*, 705–709; DE-A 19649359 (international patent pending); b) D. Henrichsen, B. Ernst, J. L. Magnani, W. T. Wang, B. Meyer, T. Peters, *Angew. Chem.* **1999**, *111*, 106–110; *Angew. Chem. Int. Ed.* **1999**, *38*, 98–102.
- [2] a) P. J. Hajduk, E. T. Olejniczak, S. W. Fesik, *J. Am. Chem. Soc.* **1997**, *119*, 12257–12261; b) A. Chen, M. J. Shapiro, *J. Am. Chem. Soc.* **1998**, *120*, 10258–10259; c) M. Lin, M. J. Shapiro, J. R. Wareing, *J. Org. Chem.* **1997**, *62*, 8930–8931.
- [3] S. B. Shuker, P. J. Hajduk, R. P. Meadows, S. W. Fesik, *Science* **1996**, *274*, 1531–1537.
- [4] K. Akasaka, M. Konrad, R. S. Goody, *FEBS Lett.* **1978**, *96*, 287–290.
- [5] J. D. Stoesz, A. G. Redfield, *FEBS Lett.* **1978**, *91*, 320–324.
- [6] a) K. Akasaka, *J. Magn. Reson.* **1979**, *36*, 135–140; b) L. Poppe, G. S. Brown, J. S. Philo, P. V. Nikrad, B. H. Shah, *J. Am. Chem. Soc.* **1997**, *119*, 1727–1736.
- [7] A. Kalk, H. J. C. Berendsen, *J. Magn. Reson.* **1976**, *24*, 343–366.
- [8] Unpublished data shows that the STD NMR approach gives results even where the trNOE method no longer works. The binding interaction of a complex biantennary decasaccharide with *Ricinus communis* agglutinin-120 was studied by STD NMR methods. The dissociation constant for this ligand is $K_D = 8.16 \times 10^{-9}$ as determined by Biacore measurements (Y. Shinohara, H. Sota, F. Kim, M. Shimizu, M. Gotoh, M. Tosu, Y. Hasegawa, *J. Biochem.* **1995**, *117*, 1076–1082).
- [9] a) C. S. Wright, G. E. Kellogg, *Protein Sci.* **1996**, *5*, 1466–1476; b) J. L. Asensio, F. J. Cañada, M. Bruix, C. González, N. Khair, A. Rodríguez-Romero, J. Jiménez-Barbero, *Glycobiology* **1998**, *8*, 569–577; c) C. S. Wright, *J. Mol. Biol.* **1984**, *178*, 91–104; d) K. A. Kronis, J. P. Carver, *Biochemistry* **1985**, *24*, 826–833; e) K. A. Kronis, J. P. Carver, *Biochemistry* **1985**, *24*, 834–840; f) K. A. Kronis, J. P. Carver, *Biochemistry* **1982**, *21*, 3050–3057.
- [10] All NMR experiments were performed on a Bruker Avance DRX 500 MHz spectrometer with a 5-mm inverse triple nuclear probehead. NMR samples were prepared in 99.9% D₂O (500 µL). However, the method works as well with spectra recorded in H₂O (cf. reference [12]). 1D NMR spectra were multiplied by an exponential line broadening function of 3 Hz prior to Fourier transformation. The irradiation power in all experiments was set to about 0.2 W.
- [11] a) P. Cagas, C. A. Bush, *Biopolymers* **1990**, *30*, 1123–1138; b) H. Debray, J. Montreuil, *Carbohydr. Res.* **1989**, *185*, 15–26; c) T. Weimar, T. Peters, *Angew. Chem.* **1994**, *106*, 79–82; *Angew. Chem. Int. Ed.* **1994**, *33*, 88–91; d) F. Fukumori, N. Takeuchi, T. Hagiwara, H. Ohbayashi, T. Endo, N. Kochibe, Y. Nagata, A. Kobata, *J. Biochem.* **1990**, *107*, 190–196.
- [12] The mapping of binding epitopes was shown for peptides and glycopeptides binding to the SM3 monoclonal antibody specific to cancerous mucin mucines. H. Möller, N. Öztürk, J. Taylor-Papadimitriou, H. Paulsen, B. Meyer, unpublished results.

Cobalt has long been known to have two crystal structures—close-packed hexagonal (hcp) and face-centered cubic (fcc). While both phases can coexist at room temperature, the fcc structure is thermodynamically preferred above 450 °C and the hcp phase is favored at lower temperatures.^[1] For small particles, however, the fcc structure appears to be preferred even below room temperature.^[2] The existence of fcc and hcp cobalt was first reported by Hull^[3] in 1921 after analyzing diffraction patterns of metallic powders prepared by several methods. Krainer and Robitsch^[4] reported observing new diffraction lines in samples prepared by spark erosion of bulk cobalt surfaces, but the structure was never fully established. Kajiwar et al.^[5] observed several new lines in the diffraction pattern of cobalt nanoclusters prepared by plasma evaporation and the subsequent condensation of the metal, but attributed these lines to a form polymorphous to the two known structures. Similar results are reported by Leslie-Pelecky et al.^[6] with cobalt particles prepared by the reduction of cobalt salt in solution with metallic lithium. A recent report by Respaud et al.^[7] provides some evidence for a new structure of cobalt present in small cobalt clusters produced by the decomposition of organometallic precursors, but the structure was not identified. Herein we report and identify a new stable structure for elemental cobalt.

The fcc and hcp phases of cobalt are close-packed structures that differ only in the stacking sequence of atomic planes in the 111 direction. Low activation energy for formation of stacking faults often leads to the formation of both phases in the same sample under high-temperature crystallization techniques, such as melting–crystallization and evaporation–condensation. Low-temperature solution chemistry methods, on the other hand, often yield exclusively one phase of cobalt.

We used thermal decomposition of octacarbonyldicobalt in solution in the presence of trioctylphosphane oxide (TOPO) as a coordinating ligand to prepare cobalt nanoclusters. This method provides a “clean” route for the preparation of the material since elemental cobalt is the only nonvolatile product of the reaction: $[\text{Co}_2(\text{CO})_8] \rightarrow 2\text{Co} + 8\text{CO}$. The resulting powder was highly susceptible to magnetic fields generated by a small permanent magnet, suggesting that it consisted of metallic cobalt. Transmission electron microscopy (TEM) showed that the powder consisted of roughly spherical

[*] Prof. M. G. Bawendi, D. P. Dinega
Department of Chemistry and
Center for Materials Science and Engineering
Massachusetts Institute of Technology
Cambridge MA 02139 (USA)
Fax: (+1) 617-253-7030
E-mail: mgb@mit.edu

[**] This work was supported in part by the NSF-MRSEC program (NSF-DMR-94-00334). We would like to thank Dr. Joseph Adario for assistance with X-ray diffraction experiments, and Prof. Christopher Cummins and Dr. Christopher Murray for helpful discussions.